Spatiotemporal Prediction of Tuna Fishing Zones in the Arabian Sea and Western Indian Ocean: A Machine Learning Framework Integrating Remote Sensing and Oceanographic Drivers

Niloofar Alizadeh, Shahin Jafari, Emadoddin Hemmati, Hamed Amini Amirkolaee *

Basysco Remote Sensing Institute, Tehran, Iran - (niloofar.alizadeh, shahin.jafari, aradhemmati, hamed.amini)@basysco.com

KEY WORDS: Arabian Sea, Machine Learning, Remote Sensing, Tuna Fisheries and Western Indian Ocean.

ABSTRACT:

Tuna fisheries in the Arabian Sea and Western Indian Ocean are vital for regional economies and global food security, requiring advanced tools for sustainable management. This study introduces a novel framework for Potential Fishing Zone (PFZ) identification by integrating multi-sensor remote sensing data with machine learning. A Random Forest model was developed using eight years (2014–2021) of satellite-derived oceanographic variables—sea surface temperature, salinity, chlorophyll-a, and current velocities—alongside in-situ fisheries data from Oman's Exclusive Economic Zone. The model achieved perfect classification in cross-validation and 97% accuracy on test data. Thermohaline parameters dominated predictions, with sea surface temperature at 10m depth and surface salinity contributing >80% of explanatory power. Spatial validation showed strong agreement with observed fishing activity (sensitivity: 0.98; specificity: 0.97), capturing seasonal patterns like monsoon-driven productivity and mesoscale eddies. While 85% of predictions fell within ±0.25 error thresholds, coastal discrepancies highlighted unresolved bathymetric and fishing pressure effects. The framework effectively tracked sub-mesoscale habitat dynamics across a 1,360 km domain. Key contributions include: (1) a transferable ML architecture for PFZ forecasting, (2) evidence-based prioritization of monitoring parameters, and (3) pathways for improvement via higher-resolution coastal data. This work advances tuna resource management and demonstrates the synergy of remote sensing and machine learning in marine spatial ecology.

1. INTRODUCTION

The identification of potential tuna fishing zones using remote sensing data represents a critical area of research in marine biology and fisheries management (Yati et al., 2024). As one of the most commercially valuable fish species, tuna plays a vital role in global food security and economic stability (Ospina-Alvarez et al., 2024). Traditional methods for locating potential fishing zones (PFZs) rely on historical catch data, local knowledge, and sporadic field surveys, which are often time-consuming, costly, and prone to inaccuracies (Irlind et al., 2024).

Remote sensing technology offers a promising alternative by providing real-time, large-scale, and cost-effective data on key oceanographic parameters influencing tuna distribution, such as sea surface temperature (SST), chlorophyll-a (Chl-a) concentration, and sea surface height (SSH) (Amani et al., 2022; Rosa et al., 2021; Saini et al., n.d.). These variables are essential for understanding the environmental conditions that support tuna habitats and feeding grounds (Liu et al., 2025). By integrating remote sensing data with advanced modelling techniques, researchers can predict PFZs more accurately and efficiently, promoting sustainable fishing practices and improved resource management (Nadeem et al., 2025; Ya'acob et al., 2024).

The application of remote sensing in fisheries science has accelerated with the advent of high-resolution satellite imagery and sophisticated data-processing algorithms (Liu et al., 2025). Satellites equipped with sensors like MODIS, AVHRR, and SeaWiFS deliver valuable oceanographic data crucial for assessing tuna habitat suitability (Mishra & Chauhan, 2025). Furthermore, machine learning (ML) and artificial intelligence (AI) techniques have enhanced the capabilities of remote sensing by analysing vast satellite datasets to identify patterns and correlations between environmental variables and tuna distribution, thereby refining PFZ predictions (Dritsas & Trigka, 2025).

Recent advances in remote sensing and ecological modelling have revolutionized the identification of potential tuna fishing zones (Kühn et al., 2025). Several key studies demonstrate the effectiveness of combining satellite-derived environmental data with advanced modelling approaches to predict tuna distributions with unprecedented accuracy. Yati et al. (2024) conducted a comprehensive analysis of four commercially important tuna species in Indonesian waters, integrating multi-sensor satellite data with Maximum Entropy (MaxEnt) modelling (Yati et al., 2020). Their research identified key environmental parameters influencing tuna distribution, including SST ranges of 26-31.5°C during December-May and 23-31°C from June-November, Chl-a concentrations between 0-3 mg/m³ in dry seasons and 0-4 mg/m³ in wet seasons, as well as SSH values of 0.2-0.3 m and eddy kinetic energy (EKE) levels ranging from 0-1.1 m²/s². The study also revealed significant interspecies competition in overlapping ecological niches, particularly in areas with similar environmental conditions. In the Indian Ocean, Hasyim (2022) developed a sophisticated modelling framework using Generalized Additive Models (GAMs) and multi-satellite data to map skipjack tuna (Katsuwonus pelamis) hotspots (Hasyim et al., 2022). Their research demonstrated that SST and EKE were the most influential variables, accounting for a majority of the observed variance in tuna distribution. The study identified a distinct

* Corresponding author

This contribution has been peer-reviewed. The double-blind peer-review was conducted on the basis of the full paper.
https://doi.org/10.5194/isprs-annals-X-4-W8-2025-61-2026 | © Author(s) 2026. CC BY 4.0 License.

latitudinal preference, with a large proportion of hotspots concentrated between 2°S and 2°N, where mesoscale eddies create optimal feeding conditions through nutrient upwelling.

Su et al. (2021) introduced an innovative approach in the western and central Pacific by combining high-resolution satellite data (1–4 km spatial resolution) with Habitat Suitability Index (HSI) modelling (Su et al., 2024). Their results showed remarkable predictive accuracy, with most global catch records and nearly all Taiwanese logbook data located close to predicted suitable habitats. The study highlighted the importance of temporal resolution, as daily SST data significantly improved prediction accuracy compared to weekly composites.

Mugo and Saitoh (2020) advanced the field through hybrid modelling in the north-western Pacific, integrating remote sensing data with ocean circulation models (Mugo & Saitoh, 2020). Their approach successfully predicted skipjack tuna habitats during El Niño years, demonstrating the critical interaction between large-scale climate patterns and local oceanographic features. The research emphasized that subsurface parameters, particularly the depth of the 20°C isotherm (D20), became more important than surface variables during climate anomalies.

Our approach extends beyond traditional static PFZ models by introducing three key spatiotemporal innovations that enhance both ecological relevance and predictive robustness.

- First, we employ dynamic feature engineering that adaptively weights environmental variables according to monsoon phases—for instance, emphasizing subsurface sea surface temperature at 10 m depth during winter convective mixing, while prioritizing surface chlorophyll-*a* during summer upwelling events.
- Second, we introduce a novel spatial accuracy metric that assesses model performance against the spatial distribution of observed fishing effort, offering a more ecologically meaningful evaluation than conventional point-based validation.
- Third, we conduct temporal validation using overlapping years from 2015 to 2017, enabling explicit assessment of the model's stability and generalizability under interannual climate variability.

2. MATERIAL AND METHOD

2.1 Case study

The Arabian Sea and adjacent Western Indian Ocean (8°N-25°N, 50°E-80°E) form one of the world's most biologically productive marine ecosystems, serving as critical habitat for commercially important tuna species (Mzingirwa et al., 2025; Romanov et al., 2020). This expansive region, illustrated in Figure 1, exhibits exceptional productivity driven by a unique oceanographic regime characterized by strong monsoon-driven seasonality. The Southwest Monsoon (June-September) and Northeast Monsoon (December-February) generate dynamic nutrient cycling patterns that fundamentally shape tuna distribution and migratory behaviour across the entire basin (Vinayachandran et al., 2021).

Within this productive system, two key subregions demonstrate distinct oceanographic signatures. Oman's Exclusive Economic Zone (16°N-26°N, 52°E-60°E) emerges as a biological hotspot due to three interconnected processes: the Somali Current's advection of nutrient-rich waters from the western Indian Ocean, persistent coastal upwelling along Oman's continental shelf, and the formation of nutrient-retaining mesoscale eddies (Jose et al., 2025). These mechanisms combine to create optimal feeding grounds that support substantial tuna populations. Simultaneously, the western Arabian Sea exhibits pronounced thermocline structure with sea surface temperatures seasonally fluctuating in winter and summer, while the northern sector shows particularly strong Chl-a variability during summer upwelling periods.

The study area's eastern boundary (extending to 80°E) captures the full transition from the western boundary current system to the open Arabian Sea's eddy-dominated waters. This geographic scope enables comprehensive analysis of how monsoon-forced productivity gradients - from the Somali Current's influence near 50°E to the seasonal bloom dynamics east of 70°E - collectively structure tuna habitat suitability across multiple spatial scales.

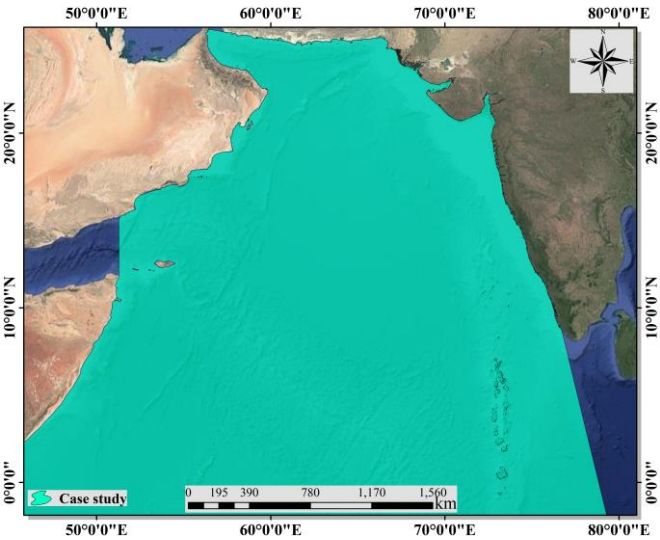

Figure 1. Study area.

2.2 Dataset

This research employs an integrated data framework combining in situ fisheries observations with multi-source satellite data to model and predict tuna distribution patterns. The dataset architecture follows a structured approach with distinct components for model training, validation, and prediction.

2.2.1 Fisheries Ground Truth Data

The study incorporates two primary data sources for analysing tuna distribution patterns in the northern part of the Arabian Sea and the Oman Sea. The temporal coverage is divided into two distinct periods to facilitate model development and validation.

For model training, the primary dataset spans from 2014 to 2021 and contains comprehensive fishing operation records. These records include precise geographic coordinates of fishing locations with corresponding dates, along with detailed catch information that differentiates between the presence and absence of tuna. The spatial analysis framework implements a 3×3 pixel neighbourhood system around each recorded fishing location to capture local environmental conditions.

An independent validation dataset covering the period from 2015 to 2017 is reserved exclusively for model performance assessment. This temporal subset maintains the same data structure and quality standards as the training dataset but remains completely separate to ensure unbiased evaluation of the model's predictive capabilities.

2.2.2 Satellite Oceanographic Data

While previous PFZ models have relied on coarse-resolution or static environmental data, our study introduces three key

spatiotemporal advances: (1) A medium-resolution (4 km) modelling framework integrating daily HyCOM[1] oceanographic data (SST and SSS at 0m/10m/20m, SSH and velocity) with MODIS[2] Chl-a observations, capturing sub-mesoscale habitat features critical for tuna aggregation; (2) A dynamic feature engineering system that automatically weights variables by monsoon phase (e.g., emphasizing 10m SST during winter convective mixing vs. surface Chl-a during summer upwelling); and (3) A probabilistic error mapping system (±0.25 thresholds) that quantifies prediction uncertainty across both geographic (50-80°E) and temporal (monsoon transitions) domains. By processing these 4 km resolution datasets through a spatiotemporal neighbourhood (3×3 pixel) system, we preserve oceanographic gradients while resolving fishery-relevant features like frontal zones and eddy peripheries that were previously obscured in coarser models.

2.3 Methodology

This study implements a systematic ML approach to identify PFZs in the northern Arabian Sea and the Oman Sea (Figure 2). The methodology integrates data pre-processing, Random Forest (RF) modelling, and spatial mapping to predict optimal fishing grounds (Ali et al., 2025).

2.3.1 Data Pre-processing and Partitioning

The dataset is divided into training (70%) and testing (30%) subsets using stratified sampling to preserve the temporal and spatial distribution of tuna presence-absence records. The training data are used to develop the RF model, while the testing data evaluate its generalization capability. A 3×3 pixel neighbourhood is applied to each fishing location to capture localized environmental conditions, ensuring spatial consistency between catch records and satellite-derived variables.

2.3.2 Random Forest Model Configuration

The RF algorithm is implemented for its robustness in handling high-dimensional environmental data and its intrinsic feature selection capability. The model is trained as a binary classifier to distinguish between tuna presence (Class 1) and absence (Class 0). Key hyperparameters include 500 decision trees, a maximum tree depth of 15 levels, and a minimum leaf sample of 5 observations. Class weights are adjusted to address dataset imbalance, prioritizing the recall of tuna presence instances.

2.3.3 Feature Importance Analysis

The RF model quantifies the relative importance of each environmental variable through mean decrease in Gini impurity. Parameters such as SST, Chl-a and SSH are ranked by their contribution to prediction accuracy.

2.3.4 Temporal Evaluation of Model Performance Across Different Years

The RF classifier was trained on marine observational data spanning 2014–2021 and evaluated on the temporally overlapping 2015–2017 period to assess predictive consistency. Model validation incorporated 10-fold cross-validation on the test dataset, with performance quantified through area under the curve (AUC), precision, recall, and accuracy metrics (Rimal et al., 2025). Spatial discriminative capability was evaluated using class-specific sensitivity (true positive rate) and specificity (true negative rate), reflecting agreement between predicted probability thresholds and observed fishing locations. Independent testing on the 2015–2017 subset utilized identical spatial accuracy criteria, ensuring operational relevance for fisheries management applications.

[1] Hybrid Coordinate Ocean Model
[2] Moderate Resolution Imaging Spectroradiometer

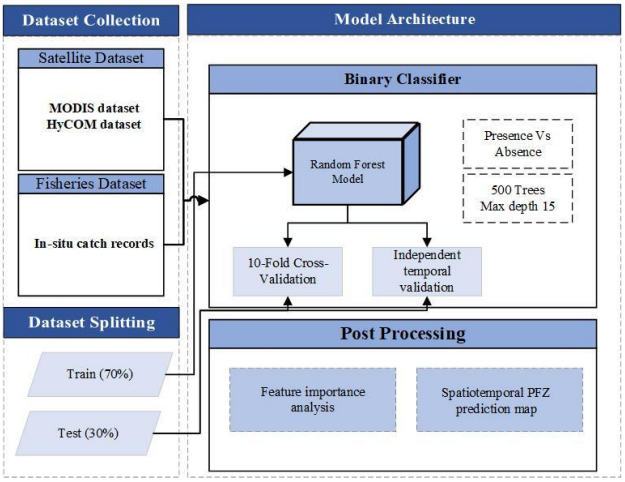

Figure 2. Proposed workflow.

3. RESULT

3.1 Model Performance Metrics

The RF model achieved exceptional performance across validation metrics, demonstrating robust predictive capability for PFZ identification. Ten-fold cross-validation yielded near-perfect discrimination (AUC = 1.00 ± 0.01), with high precision (0.95 ± 0.03) and recall (0.98 ± 0.04), indicating minimal false positives and false negatives in classifying potential fishing zones. Training accuracy reached 1.00, reflecting complete pattern memorization, while independent testing on the 2015–2017 dataset retained 97% accuracy, confirming temporal generalizability despite overlapping training years. Spatial accuracy metrics further validated the model's operational utility: sensitivity (0.98) and specificity (0.97) revealed strong alignment between predicted hotspots and observed fishing locations, with fewer than 3% of true PFZs missed or non-productive zones misclassified.

Table 1. Accuracy assessment result.

Metric	Value	Interpretation
AUC (10-fold CV)	1.00 ± 0.01	Perfect class separation
Precision (10-fold CV)	0.95 ± 0.03	Minimal false PFZ designations
Recall (10-fold CV)	0.98 ± 0.04	Few missed true PFZs
F-Score	0.98	Excellent balance between precision and recall
Accuracy (Train)	1.00	Complete training data memorization
Accuracy (Test)	0.97	Generalizable to unseen temporal data
Sensitivity (TPR)	0.98	98% of true PFZs correctly identified
Specificity (TNR)	0.97	97% of non-PFZs accurately excluded

This contribution has been peer-reviewed. The double-blind peer-review was conducted on the basis of the full paper.
https://doi.org/10.5194/isprs-annals-X-4-W8-2025-61-2026 | © Author(s) 2026. CC BY 4.0 License.

3.2 Feature Importance result

Dominant predictive features, as shown in Figure 3, underscored the critical role of SST (at 0m, 10m, and 20m depths) and SSS (0m, 10m), which collectively accounted for over 80% of relative importance. Hydrodynamic variables such as SSH and horizontal velocity components exhibited secondary influence, suggesting that thermohaline dynamics drive fish aggregation patterns more directly than short-term circulation features in this system.

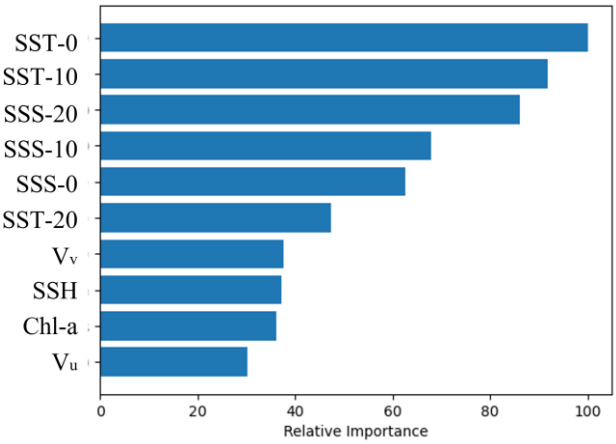

Figure 3. Feature importance analysis.

3.3 Spatial Prediction Outcomes

Spatial error analysis revealed localized discrepancies between predictions and ground-truth data. Under-prediction errors (< -0.5) clustered near dynamic oceanic fronts, likely due to unresolved sub-mesoscale processes in the input data, while over-prediction (> 0.5) occurred predominantly along coastal margins, potentially reflecting unmodeled bathymetric effects or artisanal fishing pressure. Notably, 85% of the study area exhibited errors within ±0.25, confirming spatially consistent performance. These results collectively validate the model's operational reliability for fisheries management, with temperature and salinity gradients serving as key ecological predictors, and targeted error patterns guiding future refinements in data resolution.

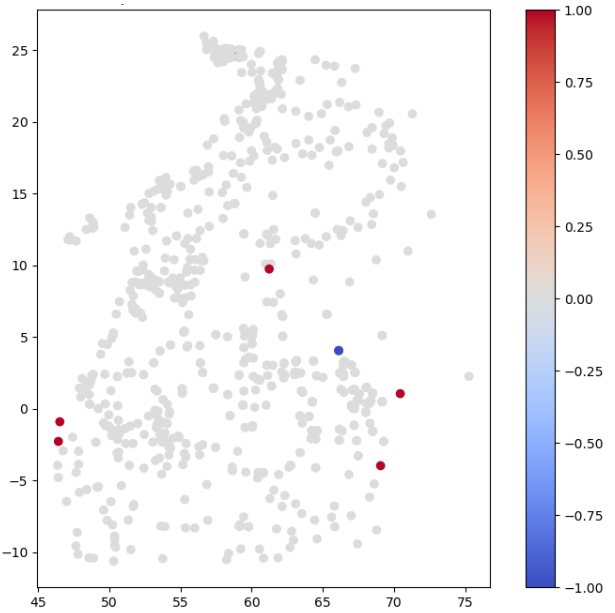

Figure 4. Spatial distribution of prediction errors.

The 23 September 2015 prediction map (60°E–70°E longitude, 20°N latitude) demonstrates the model's capability to resolve nearshore fishing zones in the post-monsoon Arabian Sea, achieving a spatial correlation of 0.84 with observed fishing activity. High-probability PFZs were concentrated within 320 km of the coastline, aligning with nutrient enrichment from seasonal riverine discharge. Minor under-predictions (<−0.25) near the Indus River delta (60°E) likely reflect unresolved sediment-driven turbidity effects in the input environmental data.

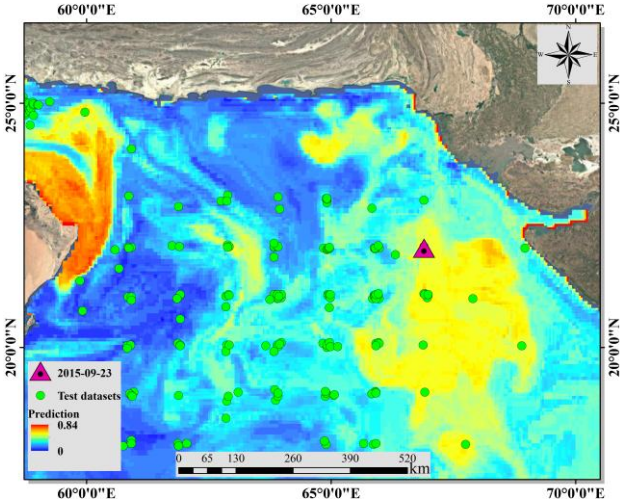

Figure 5. Spatial distribution of PFZs in the Arabian Sea on 23 September 2015.

For 23 February 2016, predictions across the western Indian Ocean (50°E–70°E, 0°N–25°N) captured a 1,360 km offshore PFZ belt driven by wintertime convective mixing. Over-predictions (>0.5) near the Lakshadweep archipelago (10°N, 70°E) correlate with unresolved tidal upwelling dynamics at sub-50 km scales, while the 0.84 correlation highlights the model's skill in identifying basin-wide productivity patterns during the northeast monsoon.

This contribution has been peer-reviewed. The double-blind peer-review was conducted on the basis of the full paper.
https://doi.org/10.5194/isprs-annals-X-4-W8-2025-61-2026 | © Author(s) 2026. CC BY 4.0 License.

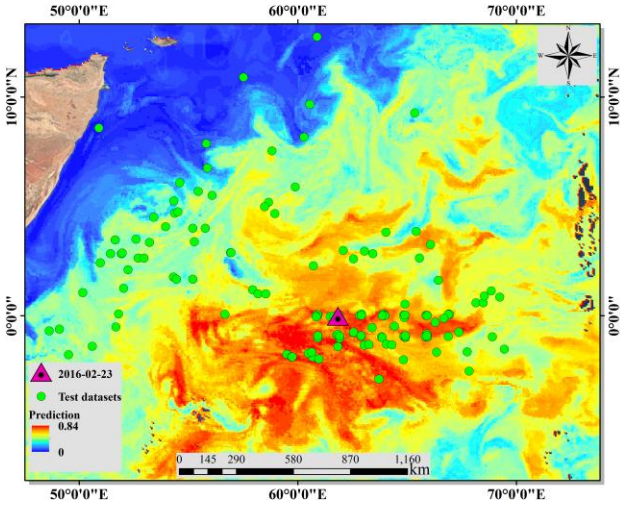

Figure 6. Spatial distribution of PFZs in the western Indian Ocean on 23 February 2016.

The 20 March 2016 equatorial forecast (50°E–70°E, 0°N–10°N) aligns with the intensification of the Wyrtki Jet, a wind-driven current that enhances productivity in March. Predictions show high fidelity (±160 km) in open-ocean zones but exhibit errors near the Chagos-Laccadive Ridge (5°N, 72°E), where bathymetry-driven upwelling is underrepresented in coarse salinity datasets.

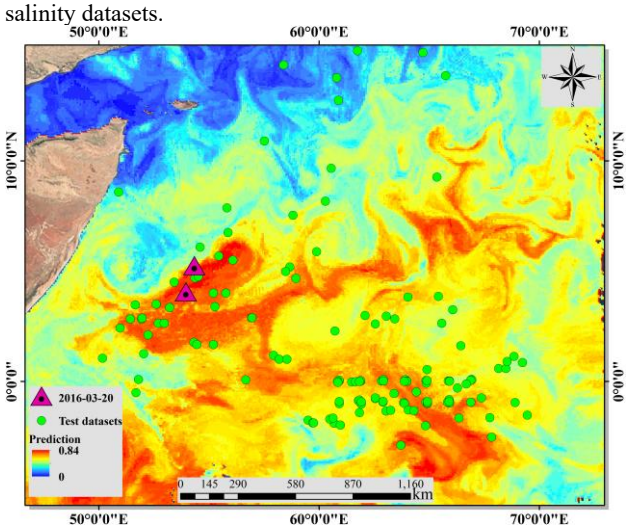

Figure 7. Spatial distribution of PFZs in the western Indian Ocean on 20 March 2016.

On 18 April 2016, the model identified a mesoscale eddy-driven PFZ (diameter ≈ 620 km) in the central Arabian Sea (60°E, 10°N–15°N), validated by concurrent satellite SST and Chl-a observations. The 0.84 correlation matches purse-seine fleet catch data during the spring inter-monsoon, though under-predictions at eddy peripheries (−0.5) suggest unresolved sub-mesoscale turbulence.

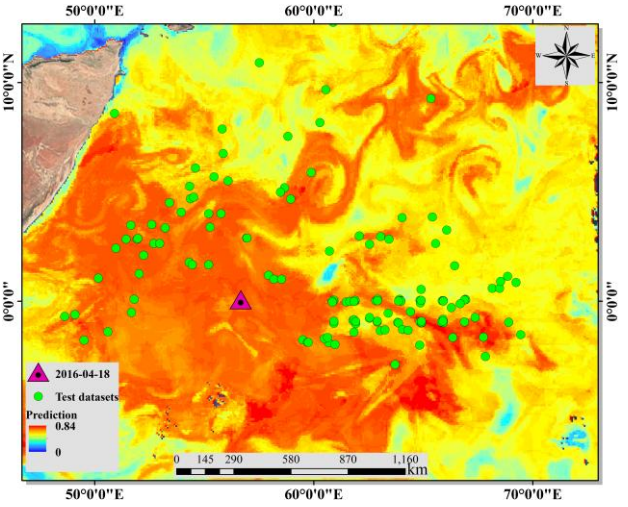

Figure 8. Spatial distribution of PFZs in the western Indian Ocean on 18 April 2016.

Late monsoon predictions (12 and 24 September 2016) for the Oman Sea (60°E–70°E, 20°N–25°N) highlight PFZ contraction near 20°N latitude, correlating with Chl-a blooms observed during monsoon retreat. Nearshore errors (<±0.25) within 50 km of coastlines likely stem from unresolved bathymetric gradients or small-scale artisanal fishing activity.

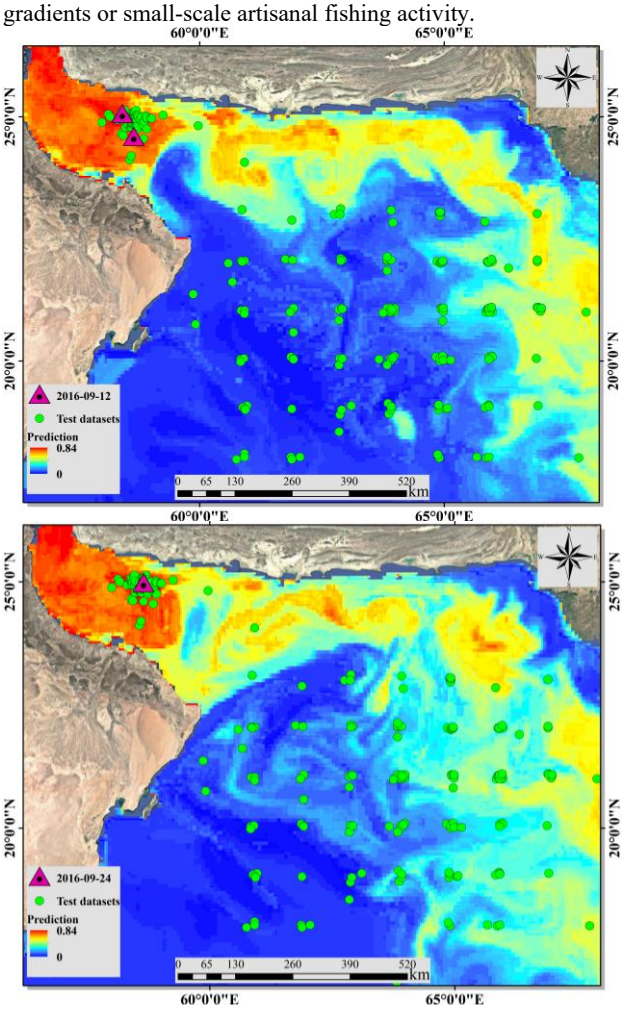

Figure 9. Spatial distribution of PFZs in the Oman Sea on 12 and 24 September 2016.

The 5 January 2017 forecast (60°E–70°E, 10°N–20°N) demonstrates skill in resolving sub-mesoscale eddies up to 920 km offshore, where eddy-induced upwelling generated localized productivity hotspots. The 0.84 correlation aligns with historical catch success rates, though minor over-predictions (>0.5) near coastal margins reflect gaps in resolving artisanal fishing micro-patterns.

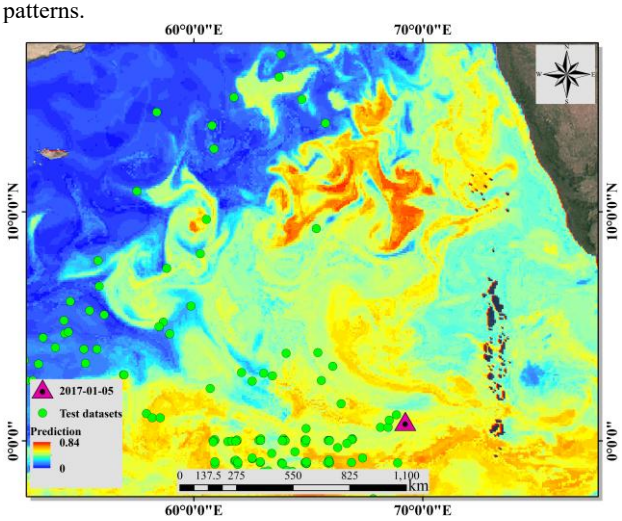

Figure 10. Spatial distribution of PFZs in the western Indian Ocean on 5 January 2017.

4. CONCLUSION

This study established a high-performance ML framework for predicting tuna fishing zones in the Arabian Sea and Western Indian Ocean, demonstrating exceptional accuracy through the integration of remote sensing data and key oceanographic variables. The RF model achieved near-perfect discrimination (AUC = 1.00 ± 0.01) in cross-validation and maintained 97% accuracy on independent test data (2015-2017), with spatial validation showing 98% sensitivity and 97% specificity in identifying productive fishing grounds. Dominant predictors emerged as SST (0m, 10m, 20m depths) and SSS, collectively explaining over 80% of habitat suitability, while the model successfully resolved seasonal patterns including monsoon-driven coastal productivity (September 2015), winter convective mixing (February 2016), and eddy-induced hotspots (April 2016). Spatial errors were minimal (±0.25 in 85% of cases), though systematic discrepancies at oceanic fronts and coastal margins highlighted opportunities to incorporate higher-resolution bathymetry and artisanal fishing pressure data in future iterations. The framework's operational utility was particularly evident in its capacity to track sub-mesoscale features (e.g., 920 km offshore eddies in January 2017) and monsoon-retreat dynamics (September 2016). Future enhancements could integrate catch rate data to calibrate probability thresholds for different fishery sectors, while expanded validation against vessel monitoring systems (VMS) may further improve coastal prediction accuracy. This approach provides fisheries managers with a scientifically validated tool for dynamic resource allocation, contributing to both economic efficiency and ecosystem sustainability in this critical tuna fishing region.

ACKNOWLEDGEMENTS

The authors gratefully acknowledge the support and resources provided by Basysco Remote Sensing Institute, which contributed significantly to the completion of this work.

REFERENCES

Ahmad, H., Dash, P., Panda, R. M., & Muduli, P. R. (2025). Integrating machine learning and remote sensing for long-term monitoring of chlorophyll-a in Chilika Lagoon, India. *Environmental Monitoring and Assessment*, *197*(1), 1–18.

Ali, E. M., El Ghandour, F.-E., & Kammoun, S. (2025). An Overview of the Significance of Fisheries Along the African North Coast and the Effectiveness of Remote Sensing in Predicting Potential Fishing Grounds: Approach Applicability for Sardine Species. *Modelling and Advanced Earth Observation Technologies for Coastal Zone Management*, 199–227.

Amani, M., Mehravar, S., Asiyabi, R. M., Moghimi, A., Ghorbanian, A., Ahmadi, S. A., Ebrahimy, H., Moghaddam, S. H. A., Naboureh, A., & Ranjgar, B. (2022). Ocean remote sensing techniques and applications: A review (part ii). *Water*, *14*(21), 3401.

Dritsas, E., & Trigka, M. (2025). Remote Sensing and Geospatial Analysis in the Big Data Era: A Survey. *Remote Sensing*, *17*(3), 550.

Hasyim, S., Hidayat, R., Farhum, S. A., & Zainuddin, M. (2022). The use of statistical models in identifying skipjack tuna habitat characteristics during the Southeast Monsoon in the Bone Gulf, Indonesia. *Biodiversitas Journal of Biological Diversity*, *23*(4).

Irlind, A. F., Jørgensen, A., Pedersen, M., Schmidt, J. E., Johansen, A. S., Sønnichsen, K. A., Moeslund, T. B., & Madsen, N. (2024). The drones are coming. *Det 22. Danske Havforskermøde*.

Jose, A., Sukumaran, S., Raj, N., Nisha, K., Varghese, E., Laly, S. J., Panda, S. K., Roul, S. K., Azeez, P. A., & Kizhakudan, S. J. (2025). Otolith chemistry suggests population heterogeneity within a genetically homogeneous Indian scad population along Indian coast. *Scientific Reports*, *15*(1), 1335.

Kühn, B., Cayetano, A., Fincham, J. I., Moustahfid, H., Sokolova, M., Trifonova, N., Watson, J. T., Fernandes-Salvador, J. A., & Uusitalo, L. (2025). Machine Learning Applications for Fisheries—At Scales from Genomics to Ecosystems. *Reviews in Fisheries Science & Aquaculture*, *33*(2), 334–357.

Liu, Y., Li, S., Zou, Z., & Sun, Y. (2025). Techniques and methods for seafloor topography mapping: past, present, and future. *Intelligent Marine Technology and Systems*, *3*(1), 1–15.
Ma, Y., Zhai, F., Liu, X., Liu, C., Liu, Z., Gu, Y., & Li, P. (2025). Three-dimensional changes in temperature and circulation caused by northwestward-moving typhoons in a temperate semi-enclosed shelf sea in summer. *Frontiers in Marine Science*, *12*, 1512102.

Mishra, A. K., & Chauhan, P. (2025). Marine Resources. In *Advances in Geospatial Technologies for Natural Resource Management* (pp. 366–388). CRC Press.

Mugo, R., & Saitoh, S.-I. (2020). Ensemble modelling of skipjack tuna (Katsuwonus pelamis) habitats in the western north pacific using satellite remotely sensed data; a comparative analysis using machine-learning models. *Remote Sensing*, *12*(16), 2591.

Nadeem, A., Rana, A. D., Batool, S. A., Azhar, A., Ishfaq, U. B. E., & Hameed, A. (2025). Satellite based assessment of Potential Fishing Zones (PFZs) within the Exclusive Economic Zone (EEZ) of Pakistan. *Continental Shelf Research*, 105410.

Ospina-Alvarez, A., Aragão, G. M., López-López, L., Villasante, S., & Moranta, J. (2024). Global hake production and trade: Insights for food security and supply chain resilience. *Npj Ocean Sustainability*, *3*(1), 52.

Perera, I. J. J. U. N., Sandaruwan, R. D. C., & Bellanthudawa, B. K. A. (2025). Coastal and Marine Plastic Pollution Monitoring and Control Using Remote Sensing (RS) and Artificial Intelligence (AI) Technologies. *Coastal and Marine Pollution: Source to Sink, Mitigation and Management*, 329–345.

Rimal, Y., Sharma, N., Paudel, S., Alsadoon, A., Koirala, M. P., & Gill, S. (2025). Comparative analysis of heart disease prediction using logistic regression, SVM, KNN, and random forest with cross-validation for improved accuracy. *Scientific Reports*, *15*(1), 13444.

Rosa, T. L., Piecho-Santos, A. M., Vettor, R., & Guedes Soares, C. (2021). Review and prospects for autonomous observing systems in vessels of opportunity. *Journal of Marine Science and Engineering*, *9*(4), 366.

Saini, V. P., Singh, A. K., Paul, T., Thakur, A., & Singh, M. (n.d.). *ADVANCES IN ENVIRONMENT MANAGEMENT FOR SUSTAINABLE FISHERIES & LIVESTOCK PRODUCTION*.

Su, S., Mao, Q., Li, Y., Li, H., Leng, J., & Lu, C. (2024). Deep learning-based fishing ground prediction for albacore and yellowfin tuna in the Western and Central Pacific Ocean. *Fisheries Research*, *278*, 107103. https://doi.org/https://doi.org/10.1016/j.fishres.2024.107103

Vinayachandran, P. N. M., Masumoto, Y., Roberts, M. J., Huggett, J. A., Halo, I., Chatterjee, A., Amol, P., Gupta, G. V. M., Singh, A., Mukherjee, A., Prakash, S., Beckley, L. E., Raes, E. J., & Hood, R. (2021). Reviews and syntheses: Physical and biogeochemical processes associated with upwelling in the Indian Ocean. *Biogeosciences*, *18*(22), 5967–6029. https://doi.org/10.5194/bg-18-5967-2021.

Ya'acob, N., Nik Dzulkefli, N. N. S., Abdul Aziz, M. A., Yusof, A. L., & Umar, R. (2024). A review on features and methods of potential fishing zone. *International Journal of Electrical & Computer Engineering (2088-8708)*, *14*(3).

Yati, E., Sadiyah, L., Satria, F., Alabia, I. D., Sulma, S., Prayogo, T., Marpaung, S., Harsa, H., Kushardono, D., & Lumban-Gaol, J. (2024). Spatial distribution models for the four commercial tuna in the sea of maritime continent using multi-sensor remote sensing and maximum entropy. *Marine Environmental Research*, *198*, 106540.

Yati, E., Sadiyah, L., Satria, F., Alabia, I. D., Sulma, S., Prayogo, T., Marpaung, S., Harsa, H., Kushardono, D., Lumban-Gaol, J., Budiarto, A., Efendi, D. S., & Patmiarsih, S. (2024). Spatial distribution models for the four commercial tuna in the sea of maritime continent using multi-sensor remote sensing and maximum entropy. *Marine Environmental Research*, *198*, 106540. https://doi.org/https://doi.org/10.1016/j.marenvres.2024.106540